Control of Convective Dissolution by Chemical Reactions: General Classification and Application to CO₂ Dissolution in Reactive Aqueous Solutions

V. Loodts, C. Thomas, L. Rongy, and A. De Wit

Nonlinear Physical Chemistry Unit, Service de Chimie Physique et Biologie Théorique, Faculté des Sciences, Université libre de Bruxelles (ULB), CP231, 1050 Brussels, Belgium

In partially miscible two-layer systems within a gravity field, buoyancy-driven convective motions can appear when one phase dissolves with a finite solubility into the other one. We investigate the influence of chemical reactions on such convective dissolution by a linear stability analysis of a reaction-diffusion-convection model. We show theoretically that a chemical reaction can either enhance or decrease the onset time of the convection, depending on the type of density profile building up in time in the reactive solution. We classify the stabilizing and destabilizing scenarios in a parameter space spanned by the solutal Rayleigh numbers. As an example, we experimentally demonstrate the possibility to enhance the convective dissolution of gaseous CO_2 in aqueous solutions by a classical acid-base reaction.

Can chemical reactions increase the dissolution rate of a fluid or solid into a fluid host phase by influencing possible convective flows in that phase? How does the development of these convective flows depend on the reaction type? As an example, can reactions impact solubility trapping during CO_2 sequestration in saline aquifers or oil reservoirs by controlling convective dynamics in the water or oil phase? Such questions are emblematic of the need to better understand the influence of chemical reactions on convective dissolution in partially miscible two-phase systems, where one of the phases dissolves into the other one with a finite characteristic solubility. These systems are encountered in numerous cases: binary liquid-liquid systems [1,2], solutions separated by a semipermeable membrane [3,4], solid dissolution [5], gas transfer [6–12], crystallization [13], material science [14], and nuclear [15] technology, etc.

Convection can be observed in partially miscible systems when an unstable density stratification builds up in the gravity field upon dissolution. After some time, the contact line between the denser and the less dense regions can be destabilized in the form of buoyancy-driven fingering. While the impact of chemical reactions on such fingering has already been largely studied in both miscible [16,17] and immiscible systems [18], their influence on convective dissolution in partially miscible systems remains largely unexplored.

Citri *et al.* already suggested that reactions could modify the density profile in the host phase of partially miscible systems, which could trigger hydrodynamic instabilities [1]. Recently, Budroni *et al.* have studied both experimentally and numerically the convective dissolution of an ester partially miscible into a lower denser aqueous phase [2]. They have shown that a reaction of the dissolved ester with a base in the water phase delays the onset of convection. Similarly, in the context of CO_2 capture or sequestration,

convection sets in when the top less dense CO_2 dissolves into the lower oil or aqueous phase and increases its density. Wylock *et al.* have shown that reactions of CO_2 dissolving in aqueous solutions of $NaHCO_3$ and Na_2CO_3 [10] or of some amines [11] can change the density profile in the water phase. In addition, theoretical works have shown that a reaction between dissolved CO_2 and a solid porous matrix delays the onset of convection as the reaction consumes the dissolved CO_2, thereby decreasing the unstable density gradient [19–21]. It has been suggested that density changes due to the consumption of CO_2 are not the only effects of the reaction: variations in concentrations of other dissolved species might also affect density, and thus convection [19]. These variations are, however, typically ignored in modeling [22–24]. Reactions appear thus as being able to influence convective dissolution but there is still a lack of general understanding on how a given chemical reaction can stabilize the flow and how, on the contrary, it can enhance flow motions favoring mixing of the two partially miscible phases.

In this context, we provide a general theoretical classification of the influence of $A + B \rightarrow C$ reactions on buoyancy-driven instabilities induced by dissolution in partially miscible systems. Our objective is to understand how the convective dissolution of one phase into another one can be tuned by reactions. To do so, we analyze the solutions of an incompressible flow equation coupled to reaction-diffusion-convection (RDC) equations for the concentration fields in the host liquid phase. We show that, if B and C have the same diffusion coefficient, two different types of reaction-diffusion (RD) density profiles can develop in the host phase. On the basis of a linear stability analysis, we demonstrate that, when a nonmonotonic density profile with a minimum builds up in time, reactions stabilize convection. On the contrary, convection

can be accelerated in reactive systems with monotonic profiles, provided the product C of the reaction is sufficiently denser than the reactant B. We classify the stabilizing and destabilizing cases in the parameter space spanned by the solutal Rayleigh numbers. The stabilizing scenario has already been observed in experiments [2]. We experimentally demonstrate the destabilizing scenario with the dissolution of gaseous CO_2 into a lower denser aqueous solution of NaOH. The growth rate of the convection increases with the concentration of NaOH.

We consider that two partially miscible phases are in contact in a statically stable initial stratification along a horizontal flat interface at $z = 0$ with z the vertical axis, pointing downwards in the gravity field $\mathbf{g}$, and y the horizontal direction. We assume that there is a local equilibrium between both phases, so that the upper pure phase A dissolves instantaneously with a constant solubility A_0 at the top boundary of the lower denser phase, in which a reactant B is present with an initial concentration B_0. The value A_0 is here not diffusion limited but solubilization limited, and can be calculated from a partitioning law relevant to the system under study. The reaction $A + B \rightarrow C$ takes place with a kinetic constant q in the host phase. We suppose that B, C and the lower phase solvent are insoluble in A and we therefore model the dynamics in the host phase only ($z \geq 0$). We assume that its volume does not change significantly with dissolution of A and that heat effects are negligible [25].

To describe the dynamics in the lower phase, RDC equations for the concentrations $\tilde{A}$, $\tilde{B}$, and $\tilde{C}$ are coupled to a flow equation for the velocity field $\tilde{\mathbf{u}} = (\tilde{u}, \tilde{v})$ via a state equation for the solution density $\tilde{\rho}$ [26–28]:

$$\tilde{\nabla}\,\tilde{p} = -\frac{\mu}{\kappa}\tilde{\mathbf{u}} + \tilde{\rho}\mathbf{g}; \qquad \tilde{\nabla}\cdot\tilde{\mathbf{u}} = 0, \tag{1a}$$

$$\frac{\partial \tilde{A}}{\partial \tilde{t}} + (\tilde{\mathbf{u}} \cdot \tilde{\nabla})\tilde{A} = D_A\tilde{\nabla}^2\tilde{A} - q\tilde{A}\,\tilde{B}, \tag{1b}$$

$$\frac{\partial \tilde{B}}{\partial \tilde{t}} + (\tilde{\mathbf{u}} \cdot \tilde{\nabla})\tilde{B} = D_B\tilde{\nabla}^2\tilde{B} - q\tilde{A}\,\tilde{B}, \tag{1c}$$

$$\frac{\partial \tilde{C}}{\partial \tilde{t}} + (\tilde{\mathbf{u}} \cdot \tilde{\nabla})\tilde{C} = D_C\tilde{\nabla}^2\tilde{C} + q\tilde{A}\,\tilde{B}, \tag{1d}$$

$$\tilde{\rho} = \rho_0(1 + \alpha_A\tilde{A} + \alpha_B\tilde{B} + \alpha_C\tilde{C}). \tag{1e}$$

Without loss of generality, we use here the 2D incompressible Darcy's law (1a) as a flow equation in porous media but the results are straightforwardly applicable in three dimensions and to the Navier-Stokes equation as well. Here, $\tilde{p}$ is the pressure, ρ_0 is the density of the solvent of the host phase, and $\alpha_i = (1/\rho_0)(\partial\tilde{\rho}/\partial\tilde{i})$ is the solutal expansion coefficient of the species i. The dynamic viscosity μ, chemical rate constant q, molecular diffusion coefficients D_i, and permeability κ are assumed constant.

To obtain dimensionless equations, we use the characteristic RD scales: length $l_c = \sqrt{D_A/(qA_0)}$, time $t_c = l_c^2/D_A$, velocity $u_c = D_A/l_c$, concentration A_0, and we define a dimensionless density $\rho = (\tilde{\rho} - \rho_0)g\kappa l_c/(\mu D_A)$ [28]. Introducing the stream function Ψ, the dimensionless governing equations are

$$\nabla^2\Psi = R_A A_y + R_B B_y + R_C C_y, \tag{2a}$$

$$A_t - \Psi_z A_y + \Psi_y A_z = \nabla^2 A - AB, \tag{2b}$$

$$B_t - \Psi_z B_y + \Psi_y B_z = \delta_B\nabla^2 B - AB, \tag{2c}$$

$$C_t - \Psi_z C_y + \Psi_y C_z = \delta_C\nabla^2 C + AB, \tag{2d}$$

where $f_x = \partial f/\partial x$, $\delta_j = D_j/D_A$ and the Rayleigh numbers are defined as

$$R_j = \frac{\rho_0\alpha_j A_0 g\kappa l_c}{\mu D_A}.$$

The initial conditions are $\forall y$: $(A, B, C, \Psi) = (1, \beta, 0, 0)$ for $z = 0$ while $(A, B, C, \Psi) = (0, \beta, 0, 0)$ for $z > 0$, where $\beta = B_0/A_0$. At the upper boundary $z = 0$, we fix $A = 1$, $B_z = 0$, $C_z = 0$, $\Psi = 0$, while at $z \rightarrow +\infty$, $(A, B, C, \Psi) \rightarrow (0, \beta, 0, 0)$.

We assume that $R_A > 0$, which means that the dissolution of the upper phase A increases the density of the lower host fluid ($\alpha_A > 0$). The opposite case $R_A < 0$ [6] can be obtained straightforwardly. To focus on the effect of changes in R_B and R_C on convection and avoid any double diffusive instability [16,17], B and C are set to diffuse at the same rate ($\delta_B = \delta_C = \delta$). Adding (2c) and (2d) with the given boundary conditions leads to $C = \beta - B$, $\forall y, z, t$, so that we need to solve Eqs. (2a)–(2c) only.

The base state dimensionless density profiles are

$$\rho^s(z, t) = R_A A^s(z, t) + (R_B - R_C)B^s(z, t) + R_C\beta, \tag{3}$$

where the base state concentration profiles A^s and B^s are solutions of the reduced RD equations (2b)–(2c) with $\Psi = 0$. Note that these density profiles and, hence, the classification we propose, do not depend on the flow equation used. Figure 1 shows the nonreactive (NR) density profile $\rho_{NR}^s(z, t) = R_A[1 - \mathrm{erf}(\eta)]$, where $\eta = z/2\sqrt{t}$. It decreases monotonically between $\rho^s = R_A$ at $z = 0$ where $A^s = 1$, down to $\rho^s = 0$ at $z \rightarrow \infty$, giving the buoyantly unstable density stratification at the origin of classical density fingering [9]. Typical reactive density profiles (3) computed with asymptotic concentrations profiles [29] are plotted in Fig. 1 for a fixed R_C and different values of R_B. At large times, B has been totally consumed near the interface to produce C. The density (3) changes from $\rho^s = R_A + R_C\beta$ at $z = 0$ where $B^s = 0$, down to its bulk value $R_B\beta$ for $z \rightarrow \infty$ (Fig. 1). Note that there are no values
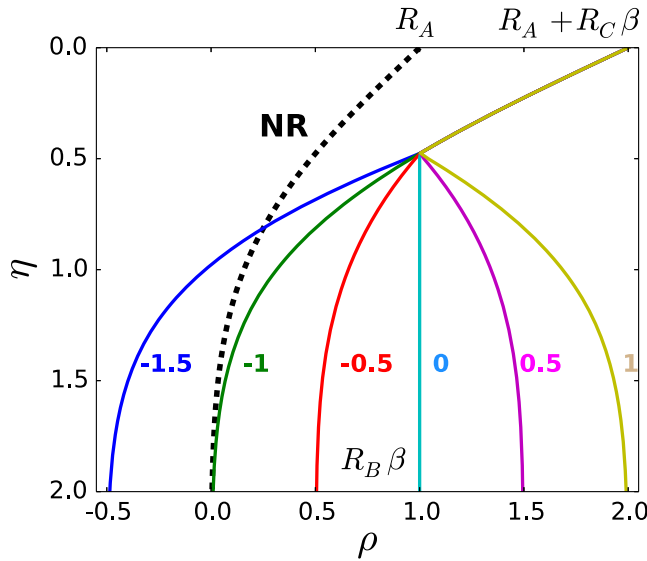
FIG. 1 (color online). Typical reactive density profiles computed using asymptotic concentration profiles with $\beta = 1$, $\delta = 1$, $R_A = 1$, $R_C = 1$, for different values of $(R_B - R_C)$ indicated at the right of each curve. The NR density profile is plotted as a dashed curve.

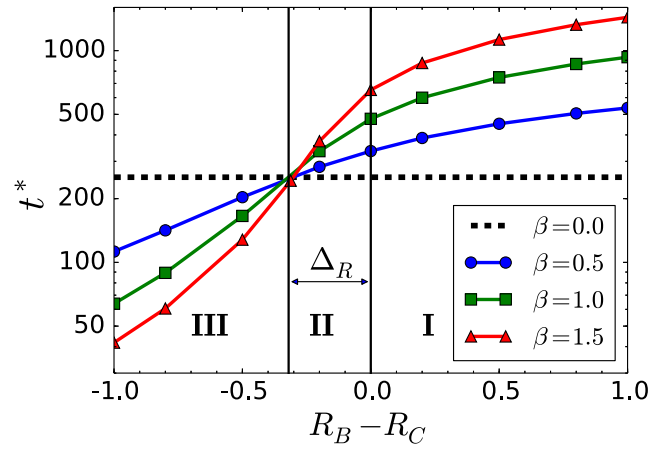
FIG. 2 (color online). Characteristic time t^* as a function of $(R_B - R_C)$, for $R_A = 1$ and $\delta = 1$. $\Delta_R > 0$ varies slightly with β (not visible on the graph).

(R_B, R_C) for which the reactive density profile is exactly the same as in the absence of reaction.

As the presence of extrema in $\rho^s(z, t)$ is known to affect the stability of the system [16,28], we next look at the region in parameter space (R_B, R_C) where ρ^s is nonmonotonic, for which its derivative relative to z,

$$\rho_z^s(z, t) = R_A A_z^s(z, t) + (R_B - R_C) B_z^s(z, t), \quad (4)$$

changes sign at a given location. A^s is the largest at the interface, where A dissolves in the host solution, and then decreases monotonically along z. By contrast, B^s is the lowest at the interface, where B is consumed by the reaction with A, and then increases monotonically along z up to its bulk value. As $A_z^s \leq 0$ and $B_z^s \geq 0$, the sign of $(R_B - R_C)$ determines whether ρ^s can have an extremum. A minimum can be obtained only if $(R_B - R_C) > 0$.

To compare the stability of the reactive density profiles with that of the nonreactive ones, we perform a linear stability analysis using the quasisteady state approximation frequently used in the case of a time-dependent base state [21,25,30,31]. Normal form perturbations $e^{\sigma t + iky}(a, b, ik\psi)(z)$ are added to the base state profiles $(A^s, B^s, 0)(z, t)$ with k the wave number and σ the growth rate of the perturbations. The resulting eigenvalue problem is solved numerically on a discrete set of points, with the second-order derivatives approximated by finite differences [25,31] with the boundary conditions $(a, b_z, \psi) = 0$ at $z = 0$ and $(a, b, \psi) \to 0$ at $z \to \infty$.

We obtain the growth rate σ of the instability as a function of the wave number k at successive times t. For

each time, we compute σ_m, the maximum growth rate, and k_m, its corresponding wave number. In order to characterize the properties of the instability as a function of $(R_B - R_C)$, we compute a characteristic time t^*, defined as the one for which $\sigma_m^* t^* = 1$, such that the amplification factor $\exp(\sigma_m^* t^*)$ of the perturbation at t^* is of order unity [31]. For the NR case, $t_{NR}^* = 252$. Figure 2 shows that there exists a critical value $\Delta_R > 0$ such that if $(R_B - R_C) < -\Delta_R$, $t^* < t_{NR}^*$ and the system is more unstable as fingers appear more quickly. On the contrary, if $(R_B - R_C) > -\Delta_R$, $t^* > t_{NR}^*$ and the system is less unstable as the onset of the instability is delayed. In both cases, increasing the amount of reactant B in the host fluid magnifies the impact of the reaction on convection. Note that Δ_R depends on all parameters of the problem (β, R_A, δ) and a full parametric study of this dependence will be performed in the future.

Figure 3 summarizes the classification and stability of the density profiles in the parameter space (R_B, R_C). If $R_C < R_B$ (region I in Figs. 2–3), density profiles are less unstable than their nonreactive counterpart as $t^* > t_{NR}^*$. These profiles are nonmonotonic with a minimum, which counteracts the full development of convection thanks to the stable barrier $\rho_z^s > 0$ in the lower part of the density profile (similarly to a stabilizing density barrier which has been shown to reduce convection during copper electrolysis [32]). In our reactive case, the amplitude of this stable barrier increases with β and $(R_B - R_C) > 0$. Even if the negative gradient ρ_z^s is larger just below $z = 0$, the weight of the denser zone at the origin of the instability is reduced because of the consumption of A (Fig. 1).

If $R_C \geq R_B$ (region II and III in Figs. 2–3), the production of C compensates the consumption of B in the evolution of ρ_z^s and density profiles are monotonic. The situation depends then on whether R_C is large enough to also compensate for the consumption of A. If $R_B \leq R_C < R_B + \Delta_R$ (region II), R_C is not large enough to fully replace the contribution of A to density, and the system remains less
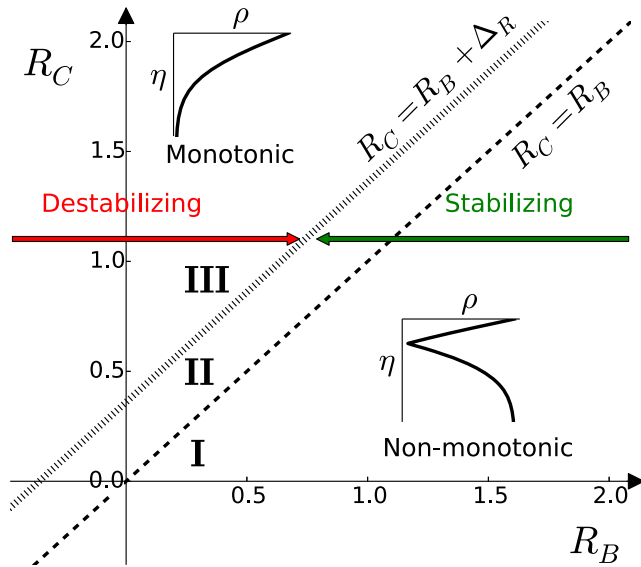
FIG. 3 (color online). Classification of the density profiles in the (R_B, R_C) parameter space for $R_A > 0$. Zone I: nonmonotonic stabilizing, zone II: monotonic stabilizing, zone III: monotonic destabilizing.

FIG. 4 (color online). Density-driven instabilities induced by dissolution of gaseous CO_2 into aqueous solutions of NaOH in increasing concentration from top to bottom shown at successive times from left to right. The field of view is 3.3 cm wide and focuses on the lower aqueous phase. The temperature is 20 °C.

unstable than without reaction ($t^* > t^*_{NR}$). If $R_C \geq R_B + \Delta_R$ (region III), the product more than compensates for the consumption of both A and B. The monotonic density profiles are then more unstable than their nonreactive counterpart as $t^* \leq t^*_{NR}$. Convection will develop faster than in the absence of reaction.

From this analysis, the strategy of a chemical control of the convective dissolution of a given species A in a bulk solvent is to choose a reactant B soluble in that solvent such that an $A + B \rightarrow C$ reaction with an appropriate $(R_B - R_C)$ value takes place in the host fluid. Varying the initial concentration ratio β allows us to tune the amplitude of the targeted stabilization or destabilization.

An example of a stabilizing strategy in region I has been evidenced recently in the convective dissolution of esters in reactive aqueous solutions of NaOH [2]. Convection develops slower and is circumscribed to a localized zone of the reactor. Another stabilizing example is the reaction of dissolved CO_2 with a porous matrix to yield a solid ($R_{B,C} = 0$, region II) [19–21]. To the best of our knowledge, a controlled *destabilization* of convection by reaction has not been demonstrated experimentally yet, despite its importance for gas transfer, solid dissolution, and CO_2 capture and sequestration, for instance. We describe below such a destabilization by a reaction between dissolved CO_2 and aqueous NaOH.

Experiments are performed in a vertically oriented Hele-Shaw cell which consists of two 20 cm × 20 cm vertical glass plates separated by a 1 mm silicone-rubber spacer. The cell is partially filled with NaOH aqueous solutions of variable concentrations and gaseous CO_2 is injected through the top of the cell to start the experiment.
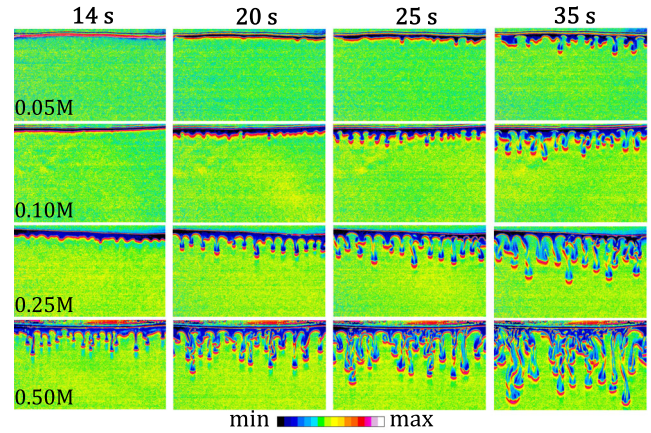
Convection in the aqueous solution is visualized with a Schlieren technique [33].

Upon dissolution in water, CO_2 reacts with NaOH to form Na_2CO_3, which has a larger solutal expansion coefficient than both reactants ($R_C \gg R_B$, destabilizing region III) [34]. Figure 4 shows the development of fingers over time [35]. Soon after the injection of CO_2, a denser CO_2-enriched boundary layer starts to develop just below the interface. This layer becomes thicker in time and is readily destabilized into fingers sinking from the interface. Over time, the fingers grow, enlarge, and penetrate deeper into the reactive solution. Precise quantitative comparison with our predictions is difficult since the detailed reactive scheme is more complex than $A + B \rightarrow C$. However, the development of the fingers is observed to be faster for more concentrated solutions (increased β), which is in agreement with our predictions.

In conclusion, we have shown that the properties of convective dissolution in partially miscible systems can be tuned by reactions of the dissolving species with properly selected chemicals present in the host fluid. Convection can be enhanced or refrained depending on whether the reaction replaces the reactants by a product sufficiently denser or not. Our classification of the reactive density profiles in the parameter space spanned by the Rayleigh numbers of the problem (Fig. 3) is valid in two and three dimensions for any flow equation. Further, we experimentally demonstrate the convective dissolution of CO_2 in aqueous solution enhanced by reaction with a base. In the context of CO_2 sequestration, our results show that an analysis of the composition and reactivity of the host liquid phase should be mandatory to select the optimal storage sites. Moreover, it demonstrates the need of taking *all* density changes induced by reactions into account in the modeling of convective dissolution to ensure better

estimations of shutdown regimes and storage capacity of sequestration sites [36]. In other applications, like gas transfer or solid dissolution, adding properly selected chemicals in the host phase would allow an active control of the instability. Further analysis of the optimum reactions for control and classification of the density profiles for different stoichiometries, reactions schemes and differential diffusion cases have been undertaken.

[1] O. Citri, M. L. Kagan, R. Kosloff, and D. Avnir, Langmuir **6**, 559 (1990).

[2] M. A. Budroni, L. A. Riolfo, L. Lemaigre, F. Rossi, M. Rustici, and A. De Wit, J. Phys. Chem. Lett. **5**, 875 (2014).

[3] D. Avnir and M. Kagan, Nature (London) **307**, 717 (1984).

[4] G. V. Rama Reddy and B. A. Puthenveettil, J. Fluid Mech. **679**, 476 (2011).

[5] A. C. Slim, M. M. Bandi, J. C. Miller, and L. Mahadevan, Phys. Fluids **25**, 024101 (2013).

[6] A. Okhotsimskii and M. Hozawa, Chem. Eng. Sci. **53**, 2547 (1998).

[7] A. Firoozabadi and P. Cheng, AIChE J. **56**, 1398 (2010).

[8] L. Rongy, K. B. Haugen, and A. Firoozabadi, AIChE J. **58**, 1336 (2012).

[9] A. Riaz, M. Hesse, H. A. Tchelepi, and F. M. Orr, Jr., J. Fluid Mech. **548**, 87 (2006).

[10] C. Wylock, S. Dehaeck, A. Rednikov, and P. Colinet, Microgravity Sci. Technol. **20**, 171 (2008).

[11] C. Wylock, S. Dehaeck, D. Alonso Quintans, P. Colinet, and B. Haut, Chem. Eng. Sci. **100**, 249 (2013).

[12] A. J. Pons, F. Sagués, M. A. Bees, and P. G. Sørensen, J. Phys. Chem. B **106**, 7252 (2002).

[13] M. Pusey, W. Witherow, and R. Naumann, J. Cryst. Growth **90**, 105 (1988); J. M. Garcia-Ruiz, M. L. Novella, R. Moreno, and J. A. Gavira, J. Cryst. Growth **232**, 165 (2001).

[14] M. Lappa, C. Piccolo, and L. Carotenuto, Colloids Surf. A **261**, 177 (2005).

[15] K. T. Kim and D. R. Olander, J. Nucl. Mater. **154**, 102 (1988).

[16] C. Almarcha, P. M. J. Trevelyan, P. Grosfils, and A. De Wit, Phys. Rev. Lett. **104**, 044501 (2010).

[17] L. Lemaigre, M. A. Budroni, L. A. Riolfo, P. Grosfils, and A. De Wit, Phys. Fluids **25**, 014103 (2013).

[18] K. Eckert and A. Grahn, Phys. Rev. Lett. **82**, 4436 (1999).

[19] J. Ennis-King and L. Paterson, Int. J. Greenhouse Gas Contr. **1**, 86 (2007).

[20] J. T. H. Andres and S. S. S. Cardoso, Phys. Rev. E **83**, 046312 (2011); Chaos **22**, 037113 (2012).

[21] K. Ghesmat, H. Hassanzadeh, and J. Abedi, J. Fluid Mech. **673**, 480 (2011).

[22] W. Zhang, Y. Li, and A. N. Omambia, Int. J. Greenhouse Gas Contr. **5**, 241 (2011).

[23] H. Tian, T. Xu, F. Wang, V. V. Patil, Y. Sun, and G. Yue, Acta Geotech. **9**, 87 (2014).

[24] T. Xu, N. Spycher, E. Sonnenthal, L. Zheng, and K. Pruess TOUGHREACT. Lawrence Berkeley National Laboratory (2012).

[25] C. Almarcha, P. M. J. Trevelyan, P. Grosfils, and A. De Wit, Phys. Rev. E **88**, 033009 (2013).

[26] Z. Neufeld and E. Hernández-García, *Chemical and Biological Processes in Fluid Flows: A Dynamical Systems Approach* (Imperial College Press, London, 2010).

[27] E. S. Oran and J. P. Boris, *Numerical Simulation of Reactive Flow* (Cambridge University Press, Cambridge, England, 2005).

[28] L. Rongy, P. M. J. Trevelyan, and A. De Wit, Phys. Rev. Lett. **101**, 084503 (2008); Chem. Eng. Sci. **65**, 2382 (2010).

[29] L. Gálfi and Z. Rácz, Phys. Rev. A **38**, 3151 (1988).

[30] C. T. Tan and G. M. Homsy, Phys. Fluids **29**, 3549 (1986).

[31] P. M. J. Trevelyan, C. Almarcha, and A. De Wit, J. Fluid Mech. **670**, 38 (2011).

[32] S. Mühlenhoff, K. Eckert, A. Heinze, and M. Uhlemann, J. Electroanal. Chem. **611**, 241 (2007).

[33] G. Settles, *Schlieren and Shadowgraph Techniques* (Springer Verlag, Berlin, 2001).

[34] At $20\,°C$, $\alpha(CO_2) = 0.00815$ L/mol, $\alpha(NaOH) = 0.0438$ L/mol, and $\alpha(Na_2CO_3) = 0.105$ L/mol, which gives for a pressure of CO_2 of 1 atm, $R_A = R_{CO_2} = 0.102$, $R_B = R_{NaOH} = 0.548$, $R_C = R_{Na_2CO_3} = 1.308$, and, thus, $R_B - R_C = -0.760$.

[35] See Supplemental Material at http://link.aps.org/supplemental/10.1103/PhysRevLett.113.114501 for a real-time movie of the convective dissolution of CO_2 at 1 atm into an aqueous solution of NaOH 0.5 M. The field of view is 3.3 cm wide. This movie corresponds to the last line of Fig. 4.

[36] D. R. Hewitt, J. A. Neufeld, and J. R. Lister, J. Fluid Mech. **719**, 551 (2013).